Journal of Power Sources 221 (2013) 64–69

Contents lists available at SciVerse ScienceDirect

Journal of Power Sources

journal homepage: www.elsevier.com/locate/jpowsour

Residual stress change with time of a segmented-in-series solid oxide fuel cell using an in situ X-ray stress measuring method

T. Somekawa*, K. Fujita, Y. Matsuzaki

Product Development Dept., Tokyo Gas Co., Ltd., 3-13-1, Minami-senjyu, Arakawa-ku, Tokyo 116-0003, Japan

HIGHLIGHTS

- We succeeded in making real-time observation of change with time of residual stress on electrolyte.
- Real-time changes with time of mechanical behaviour in anode during re-oxidation were revealed.
- In ASP-type SOFC, the destruction was observed 20 min after the beginning of re-oxidation.
- In the SIS-type SOFC, the residual stress was almost constant for more than 4 h.

ARTICLE INFO

Article history:
Received 12 April 2012
Received in revised form
5 June 2012
Accepted 21 July 2012
Available online 27 July 2012

Keywords:
Solid oxide fuel cell
Redox
Segmented-in-series
Residual stress

ABSTRACT

The changes with time of the residual stress on the electrolyte were measured in situ during re-oxidation under solid oxide fuel cell (SOFC) operation conditions using a segmented-in-series (SIS)-type SOFC and a conventional anode-supported planar (ASP)-type SOFC to understand the mechanical behaviour of the materials in the SOFC. In situ X-ray residual stress measurement was successful, and the real-time change with time of the residual stress of the electrolyte was revealed under SOFC operating conditions. In the ASP-type SOFC, the residual stress changed from compression to tensile stress, and destruction of the cell was confirmed 20 min after the air introduction. In contrast, in the case of the SIS-type SOFC, the residual stress was almost constant, even when the anode material was exposed to oxidation conditions for more than 4 h. These results indicate that the SIS-type SOFC has a high tolerance against reduction and oxidation (redox) compared with the ASP-type SOFC, which requires a conductive support material with a high Ni content. This is because the SIS-type SOFC has an electrically insulated support material that does not require a high Ni content.

1. Introduction

Recently, SOFCs have been actively developed as high-electrical-efficiency power generation equipment that utilise a limited quantity of fossil fuels [1,2]. Ensuring durability is one of most important issues for energy devices, such as SOFCs, and research into durability estimation and degrading factors is quite active. To ensure the ultralong-term durability of devices such as ceramic-based SOFCs, no destruction of the device materials can occur during the operation period. Therefore, an understanding of the mechanical behaviours caused by material properties [3–8] and inner stress, which is related to destruction of the cell under operation conditions, are needed.

Under actual load conditions, natural disasters such as earthquakes and lightning strikes, emergency stops caused by blackouts, local fuel shortages of anode material occur. These situations expose anode materials to oxidation conditions. It is well known that re-oxidation of anode materials causes expansion of the anode [9–11], which increases the residual stress on the electrolyte. As a result, the cells are destroyed by the redox reaction, and it is impossible for them to generate electricity. Therefore, redox is very significant problem, especially in the conventional ASP-type SOFC, which includes a higher concentration of NiO in the anode [12,13]. An understanding of the mechanical behaviour, such as the inner stress conditions, during redox operation is very important to design SOFCs that exhibit ultralong-term durability. Some authors have reported on the residual stress at room temperature after redox [14]. However, detailed measurements and analysis of the mechanical behaviour under SOFC operation conditions have not yet been reported.

In this study, we examined the change with time of the mechanical behaviour during redox under operation conditions by using both a conventional ASP-type SOFC and an SIS-type SOFC, which was reported to have a high redox tolerance [15–17]. The changes with time of the residual stress on the electrolyte during

* Corresponding author. Tel.: +81 3 5604 8275; fax: +81 3 5604 8051.
E-mail address: somekawa@tokyo-gas.co.jp (T. Somekawa).

0378-7753/$ – see front matter © 2012 Elsevier B.V. All rights reserved.
http://dx.doi.org/10.1016/j.jpowsour.2012.07.064

re-oxidation of the anode were examined using an X-ray diffractometer at 800 °C to understand real-time mechanical change behaviours under redox conditions.

2. Experimental

2.1. Sample preparation

2.1.1. Anode-supported planar-type SOFC

The planar-type electrode assembly ASC-27 (fuelcellmaterials.com) was used as the conventional ASP-type cell. The details of ASC-27 are shown in Table 1 and its configuration is a disk of 27 mm in diameter. In the residual stress measurements, cathodes were removed from electrolytes, and the electrolytes were irradiated with X-rays.

2.1.2. Segmented-in-series SOFC

Fig. 1 shows the schematic of an SIS-type SOFC [18,19]. In the SIS-type SOFC, multiple single cells are formed on the one electrically insulated flat support tube. The electrical current flows longitudinally up one side and back down the other side. The electrically insulating substrate is extruded in the form of a flattened tube. The anode is prepared from NiO powder and 8 mol% YSZ powder. The anode sheets are produced using a tape casting method, and they are arrayed on the substrate. Then, the substrate with the anode is dipped in a YSZ slurry, and it is fired in the electric furnace. Cathode materials are screen printed on the electrolyte and sintered. In this study, a 30 mm squared portion of the stack of the SIS-type SOFC was cut off, and the cathode materials were removed from the electrolyte. Before the residual stress measurement, both ASP-type and SIS-type samples were reduced at 800 °C for 100 h in an atmosphere of 4% H_2 balanced with N_2.

2.2. Experimental methods

2.2.1. Redox cycling tests

The redox durability of the SIS-type SOFC was evaluated. Fig. 2 shows a schematic of the experiment. An SIS-type stack was set up in the electric furnace. Both an electric current and voltage terminals were connected to the cell. The electric load was connected to the electric current terminals. The measurement of the electric current was conducted through a standard resistor. The details of the redox cycle conditions are shown in Fig. 3. The electric furnace was heated to 775 °C in 3 h in an atmosphere of 4% H_2 balanced with N_2, and then, the reduction gas was changed to 20% H_2O–H_2; this condition was maintained for 1 h. Next, the 20% H_2O–H_2 gas was stopped, and the temperature of the furnace was decreased from 775 °C to 400 °C in 1 h; this condition was maintained for 0.5 h. Finally, the supply of 20% H_2O–H_2 was restarted, and the temperature was heated from 400 °C to 775 °C in 1 h. In the redox cycling test, steps 3–6 were repeated, and the open circuit voltages (OCVs) and voltages at a current density of 0.24 A cm^{-2} at a fuel utilisation of 80% were measured.

2.2.2. In situ residual stress measurement using the X-ray stress measurement method

To investigate the mechanical behaviour during the re-oxidation, the residual stress on the electrolyte was measured using the in situ X-ray residual stress measurement method. Fig. 4 shows the experimental set up. The small-sized electric furnace, which consisted of a metal manifold and a microceramics heater, was prepared in an X-ray diffractometer device (Rigaku Corp, SmartLab), and samples were placed in the furnace. The small-sized furnace has a gas line that can supply both air and reduction gas (4% H_2 balanced with N_2). In this study, the X-ray energy was 45 keV, and a two-dimensional detector called a Pixel Apparatus for the SLS (PILATUS) was used. The detector has a 33.5 × 83.8 mm^2 detection area, the exposure time for each data point was 2.5 min and the required interval between measurements was 1 min. This was because the goniometer required 1 min to move from one measuring point to another measuring point. The reason why the PILATUS was used is that it has advantages in terms of both time resolution and measuring position reliability compared with a conventional detector; PILATUS was expected to be more suitable for the real-time analysis of the residual stress change with time.

In the furnace, the reduced samples were set and rapidly heated to 800 °C, and then, the 4% H_2 balanced with N_2 reduction gas was switched to air. The anode was re-oxidised by force at a constant temperature of 800 °C.

Table 1
The details of ASC-27.

Layer	Composition
Anode	Ni/8YSZ
Electrolyte	8YSZ
Cathode	LSM/LSM-GDC

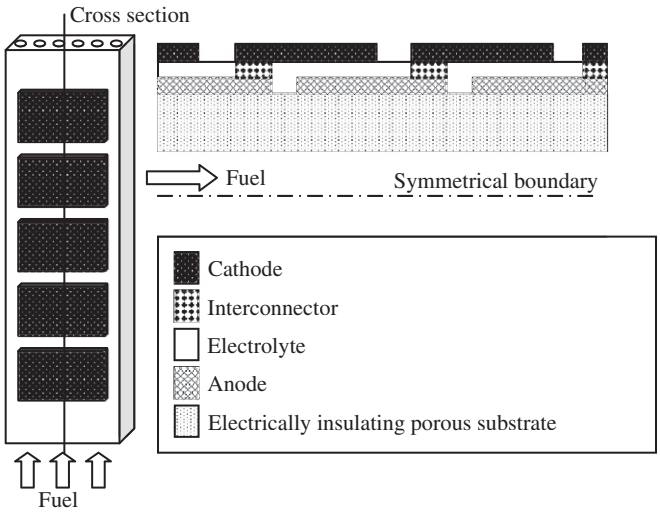

Fig. 1. Schematic of the SIS-type SOFC.

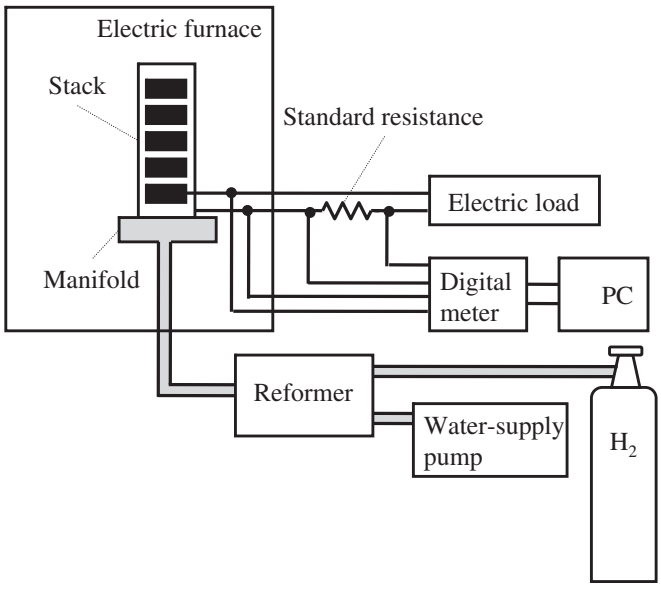

Fig. 2. Experimental set up of the redox cycling tests.

Step	Time	Temperature	Gas	Conditions
1(heating)	3.0h	RT→775°C	N_2H_2	Reduction
2(keeping)	1.0h	775°C→775°C	H_2	Reduction
3(cooling)	1.0h	775°C→400°C	(Air)	Oxidation
4(keeping)	0.5h	400°C→400°C	(Air)	Oxidation
5(heating)	1.0h	400°C→775°C	H_2	Reduction
6(keeping)	0.5h	775°C→775°C	H_2	Reduction
3-6 repeating				

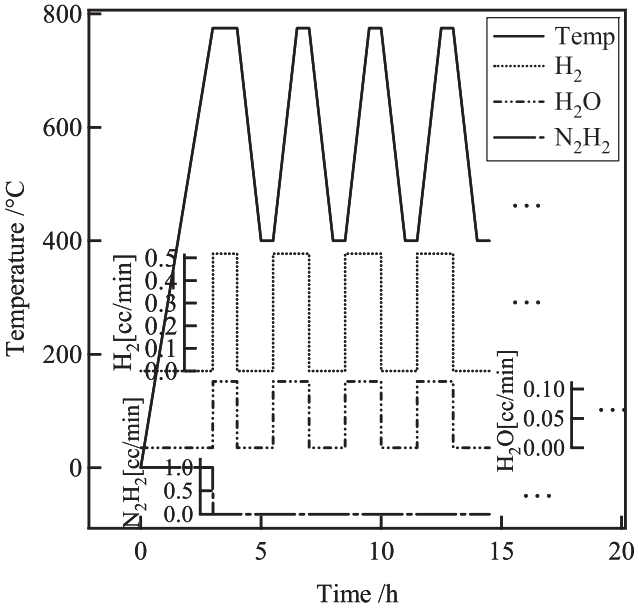

Fig. 3. The details of the redox cycling condition.

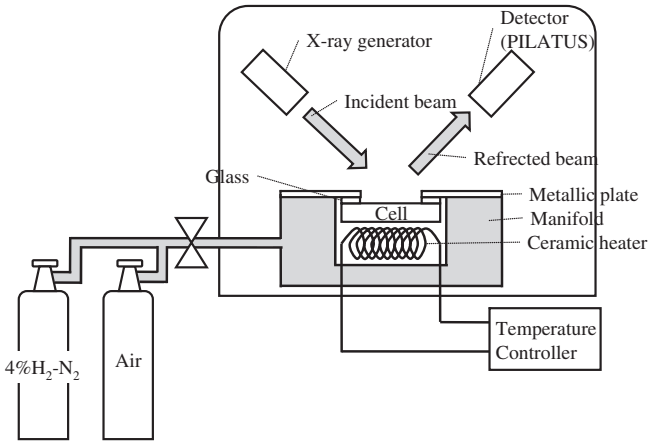

Fig. 4. Experimental set up of the in situ X-ray residual stress measurement.

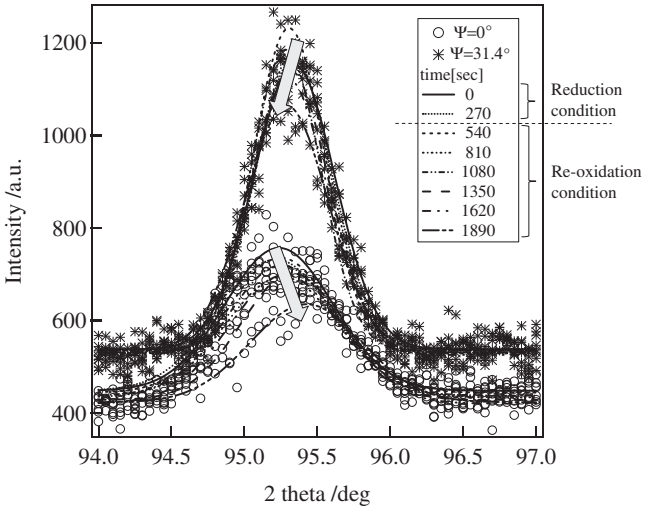

Fig. 6. The shifts of the diffraction peak position of the electrolyte in the ASP-type SOFC.

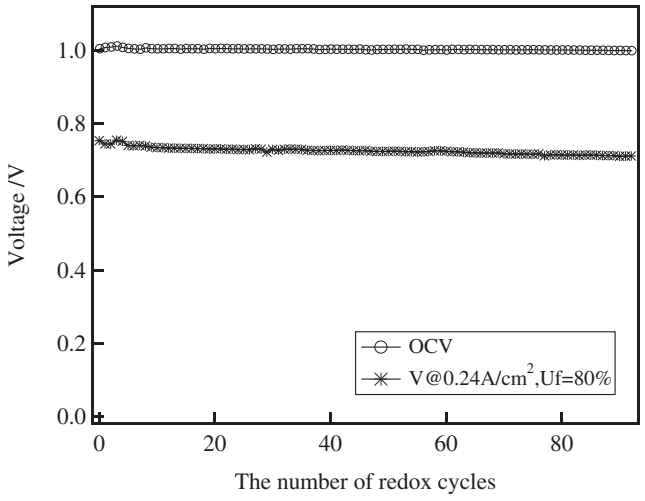

Fig. 5. The result of redox cycling tests for the SIS-type SOFC.

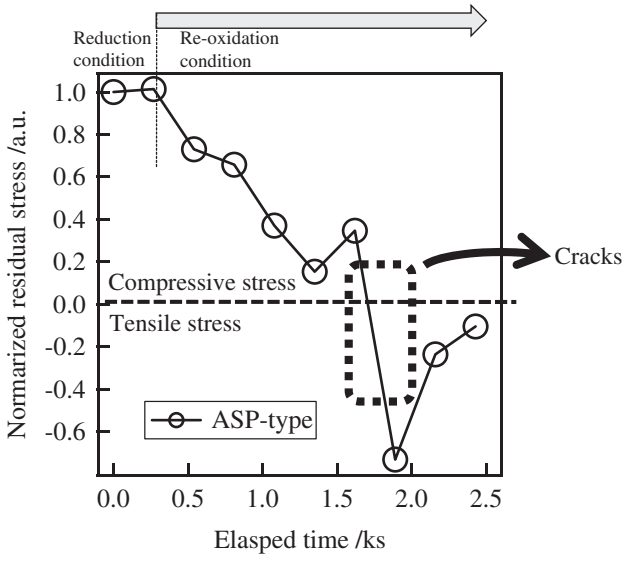

Fig. 7. The result of residual stress on the electrolyte in the ASP-type SOFC.

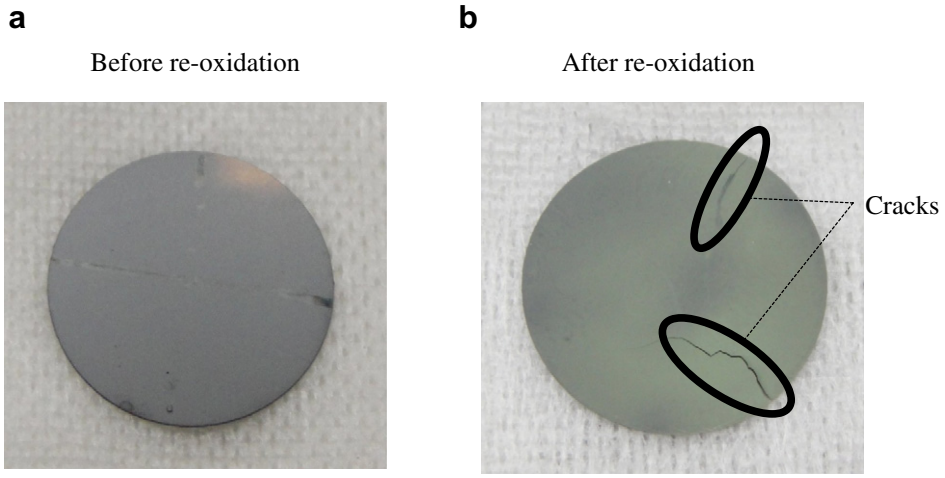

Fig. 8. The optical images of the ASP-type SOFC.

After the introduction of the air, we measured the X-ray diffraction pattern of the electrolyte of the sample and estimated the residual stress using the $\sin^2 \Psi$ method [20–24] with a concentrated-beam X-ray diffractometer equipped with a Cr target. Regarding the diffracting plane used for the stress measurement, we selected the (2 1 1) plane of YSZ. The residual stress in the electrolyte was estimated using the following formula:

$$\sigma = \frac{1}{d_0} \times \frac{E}{1+\nu} \times \frac{\partial d_\psi}{\partial \sin^2 \psi} \quad (1)$$

where d_0 is the inter-planer spacing under a stress-free condition and E and ν are Young's modulus and Poisson's ratio, respectively. Ψ is the angle between the specimen plane normal and the lattice plane normal. The gradient of the d-$\sin^2 \Psi$ diagram can be calculated by measuring the diffraction pattern at different angles of Ψ. The residual stress can be calculated.

2.2.3. SEM analysis

To analyse the microstructural changes of anodes, the cross sections near anode/electrolyte interface were observed using a scanning electron microscope (SEM, JEOL Ltd., EX-23000BU) after the re-oxidation process and cooling to room temperature.

3. Results and discussion

3.1. Redox cycling test

Fig. 5 shows the results of redox cycling tests of the SIS-type SOFC. The graph shows an almost constant value of both the OCV and the voltage at a current density of 0.24 A cm^{-2} at a fuel utilisation of 80% during 100 cycles. No remarkable damage was observed after the tests. In contrast, some authors have reported that in an ASP-type SOFC, cells can be broken even when the anode is re-oxidised only one time [25].

3.2. In situ residual stress measurement using an X-ray stress measurement method

To investigate the reason why an SIS-type SOFC has a high resistance to redox compared with a conventional ASP-type SOFC, we measured the effects of re-oxidation for the residual stress on the electrolyte and succeeded in making real-time observations of the change with time of the residual stress on the electrolyte.

Fig. 6 shows the change with time of the electrolyte peak of the (2 1 1) plane in the ASP-type SOFC. When Ψ=0°, shifts in the diffraction peak position towards higher angles were observed after air introduction. When Ψ=31.4°, shifts in the diffraction peak position towards lower angles were also observed. Fig. 7 shows the

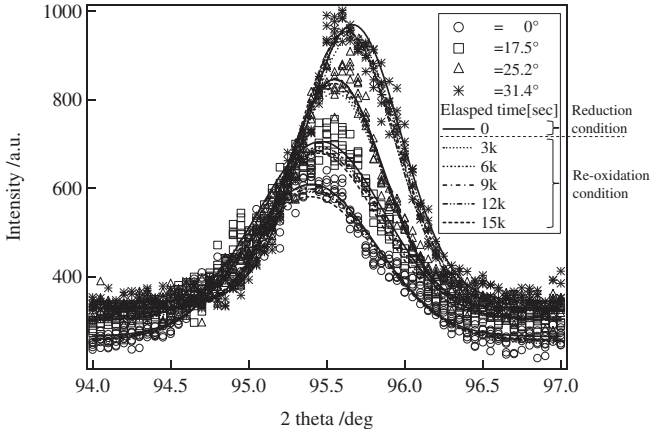

Fig. 9. The shifts of the diffraction peak position of the electrolyte in the SIS-type SOFC.

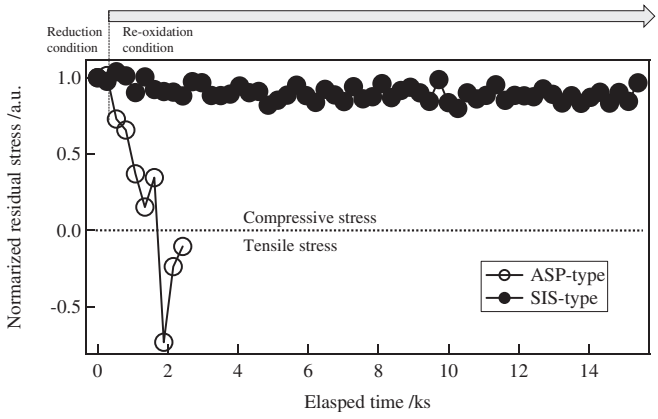

Fig. 10. The result of residual stress on the electrolyte in the SIS-type SOFC.

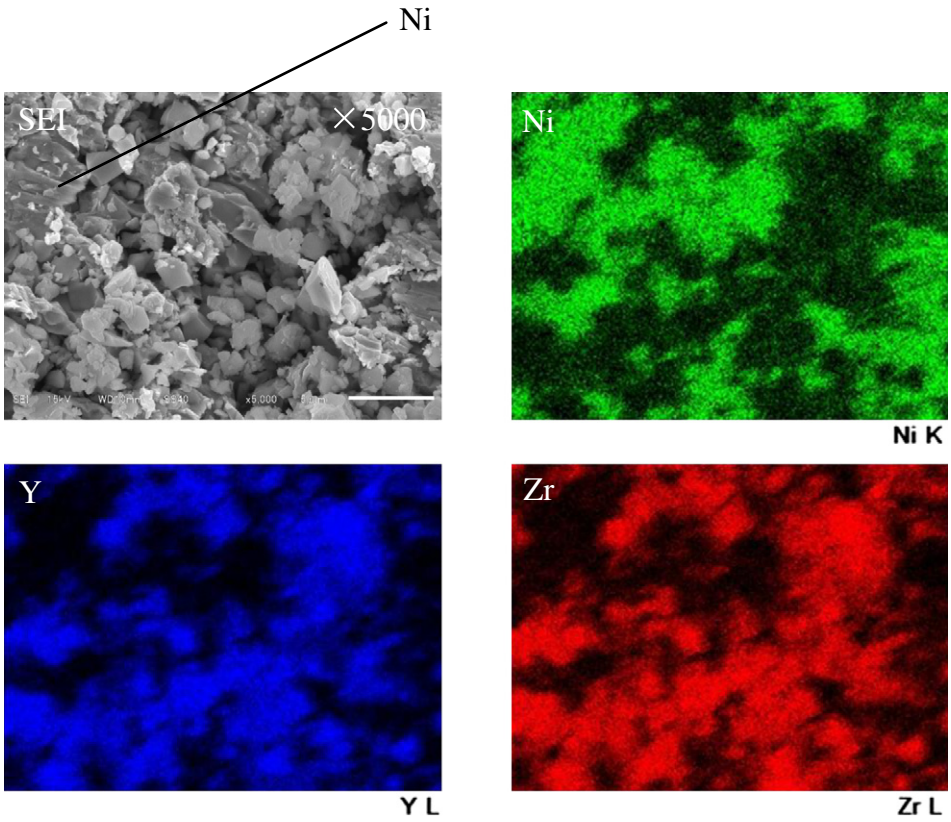

Fig. 11. SEM image and EDX results of the before re-oxidation sample of the SIS-type SOFC.

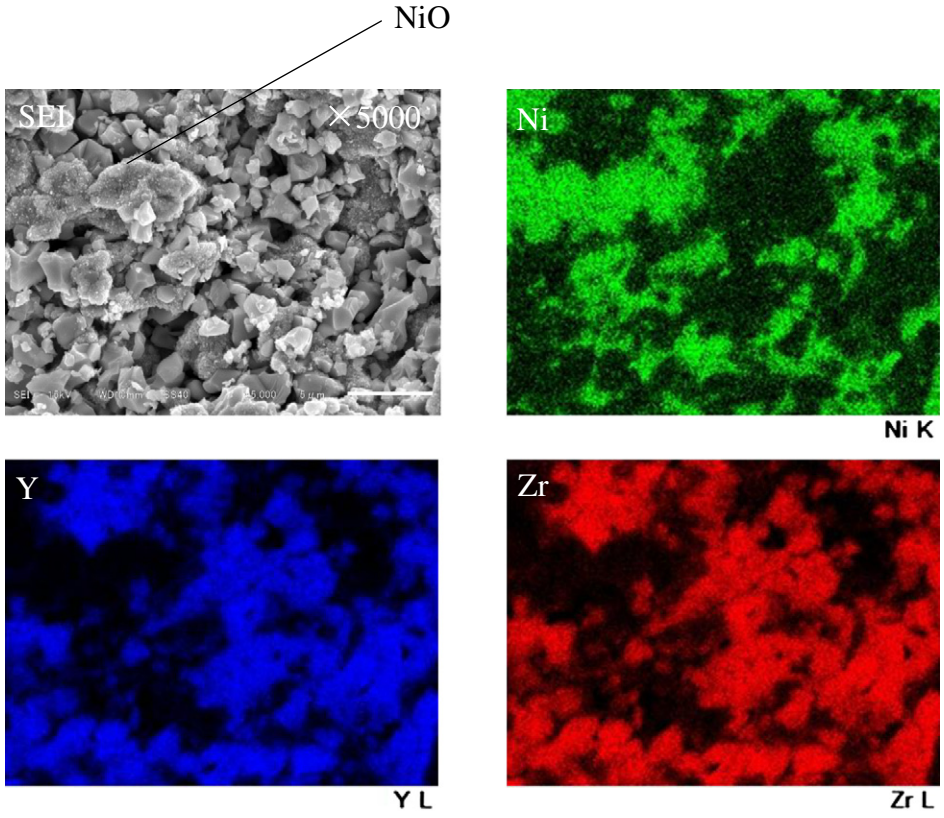

Fig. 12. SEM image and EDX results of the after re-oxidation sample of the SIS-type SOFC.

residual stress on the electrolyte calculated by using the result and formula (1). Each residual stress was normalized by the value at 800 °C under reduction condition. A positive value indicates compression stress, and a negative value indicates tensile stress. At first, under reduction conditions at 800 °C, the residual stress was a compression stress. Subsequently, the residual stresses changed from compression to tensile stress as soon as air was introduced. Twenty minutes after the air introduction, destruction of the cell was observed. Optical images of the ASP-type SOFCs are shown in Fig. 8. Fig. 8(a) shows an image before re-oxidation and (b) shows an image after re-oxidation. Fig. 8(b) shows the large cracks.

The changes with time of the diffraction peak of the (2 1 1) plane of the electrolyte in the SIS-type SOFC are shown in Fig. 9. No shifts in the diffraction peak position of the electrolyte occurred at any Ψ angles after more than 4 h since the air introduction at 800 °C had started. The calculation results of the residual stress using formula (1) are shown in Fig. 10. The residual stress remains almost constant, even after the air introduction in the SIS-type SOFC, and it has a higher stability compared with the ASP-type SOFC.

3.3. SEM analysis

Figs. 11 and 12 show the cross-sectional SEM images and EDX results of the anode in the SIS-type SOFC. Fig. 11 shows the results of before re-oxidation sample, and Fig. 12 shows the results of after re-oxidation sample. The sample of Fig. 12 was re-oxidised in the air at 800 °C for 4 h and the temperature was lowered. NiO was observed after the introduction of oxygen at 800 °C for 4 h. This finding indicates that Ni in the anode changed into NiO [25–27]. These results suggest that in the SIS-type SOFC

1) Ni in the anode is re-oxidised by the introduction of air at 800 °C,
2) The residual stress on the electrolyte is almost constant, even when re-oxidation of the Ni in the anode occurred.

These results indicate that an almost constant residual stress during the re-oxidation contributes to improvement of the mechanical resistance against redox in the SIS-type SOFC.

Next, we discuss the reason why the residual stress is kept constant. In ASP-type SOFCs, the size of anode as support material changes upon the redox treatment and the expansion of anode by the re-oxidation treatment causes the tensile stress towards the electrolyte. These macro size changes of support material cause the change of residual stress from compressive stress to tensile stress.

On the other hand, in the case of SIS-type SOFCs, as shown in Fig. 1, multiple anodes are layered on the electrically insulated substrate whose size doesn't change upon redox treatment. The chemical reaction between Ni and NiO occurs in the anode parts during redox treatment but anodes are constrained to the substrate. Compared to ASP-type SOFCs, macro size changes of the support materials of the SIS-type SOFCs don't happen. This indicates that the structure, in which the substrate prevents the anodes from changing size, relaxes the change in the residual stress of the electrolyte.

4. Conclusion

The changes with time of the residual stress on the electrolyte were measured in real time for both SIS-type SOFCs and conventional ASP-type SOFCs during re-oxidation under SOFC operation conditions to investigate the mechanical behaviours.

(a) The real-time changes with time of the mechanical behaviour in the anode during re-oxidation under SOFC operation conditions were revealed by measuring the residual stress on the electrolyte using an X-ray diffraction device.
(b) In the case of the conventional ASP-type SOFC, the residual stress on the electrolyte changed from compression to tensile stress as soon as re-oxidation started, and the destruction of the cell was observed 20 min after the beginning of re-oxidation.
(c) In the case of the SIS-type SOFC, the residual stress on the electrolyte was almost constant, even when the anode was exposed under re-oxidation conditions for more than 4 h. From the SEM analysis, it was observed that the Ni was re-oxidised into NiO.
(d) These results indicate that in the SIS-type SOFC, the lack of change of the residual stress in the electrolyte, even when Ni in the anode is re-oxidised, enhances the mechanical resistance against redox.

References

[1] H. Yokokawa, ECS Trans. 35 (1) (2011) 207–216.
[2] K. Horiuchi, K. Nakamura, Y. Matsuzaki, S. Yamashita, T. Horita, H. Kishimoto, K. Yamaji, H. Yokokawa, ECS Trans. 35 (1) (2011) 217–223.
[3] T. Kushi, S. Hashimoto, K. Amezawa, T. Kawada, K. Sato, A. Unemoto, J. Power Sources 196 (2011) 7989–7993.
[4] A. Atkinson, A. Selcuk, Solid State Ionics 134 (2000) 59–66.
[5] M. Morales, J.J. Roa, X.G. Capdevila, M. Segarra, S. Pinol, Acta Mater. 58 (2010) 2504–2509.
[6] A. Selcuk, A. Atkinson, J. Eur. Ceram. Soc. 17 (1997) 1523–1532.
[7] J.W. Adams, R. Ruh, K.S. Mazdiyasni, J. Am. Ceram. Soc. 80 (1997) 903–908.
[8] T. Hashida, K. Sato, Y. Takeyama, T. Kawada, J. Mizusaki, ECS Trans. 25 (2) (2009) 1565–1572.
[9] Manuel Ettler, Norbert H. Mezler, Hans Peter Buchkremer, Deltev Stover, Ceramic Eng. Sci. Proc. 29 (3) (2008) 33–44.
[10] T. Klemenso, C. Chung, P.H. Larsen, M. Mogensen, J. Electrochem Soc. 152 (11) (2005) A2186–A2192.
[11] T. Klemenso, F. BentSorensen, Ceramic Eng. Sci. Proc. 29 (5) (2009) 81–92.
[12] David Waldbilling, Anthony Wood, Douglas G. Ivey, Solid State Ionics 176 (2005) 847–859.
[13] V. Vedasri, J.L. Young, V.I. Briss, J. Power Sources 195 (2010) 5534–5542.
[14] K. Fujita, T. Somekawa, T. Hatae, Y. Matsuzaki, J. Power Sources 196 (2011) 9022–9026.
[15] T. Somekawa, K. Horiuchi, Y. Matsuzaki, J. Power Sources 202 (2012) 114–119.
[16] K. Fujita, T. Somekawa, K. Horiuchi, Y. Matsuzaki, J. Power Sources 193 (2009) 130–13555.
[17] T. Somekawa, K. Fujita, H. Yakabe, Y. Matsuzaki, in: Proceedings of 35th International Conference on Exposition on Advanced Ceramics and Composities, Daytona Beach, FL, USA, January 23–28, 2011, p. 40.
[18] Y. Matsuzaki, T. Hatae, S. Yamashita, ECS Trans. 25 (2) (2009) 159–166.
[19] T. Ito, Y. Matsuzaki, in: Proceedings of 34th International Conference on Exposition on Advanced Ceramics and Composities, Daytona Beach, FL, USA, January 24–29, 2010, p. 40.
[20] I.C. Noyman, J.B. Cohen, Mater. Sci. Eng. 75 (1983) 179.
[21] I.C. Noyman, J.B. Cohen, Adv. X-ray Anal. 27 (1984) 129.
[22] K. Tanaka, Y. Yamamori, N. Mine, K. Suzuki, in: Proceedings of the 32nd Japan Congress on Materials Research, 1989, p. 199.
[23] Y. Yoshioka, Adv. X-ray Anal. 24 (1981) 167.
[24] M. Barral, J.M. Sprauel, J. Lebrun, G. Maeder, S. Magtert, Adv. X-ray Anal. 27 (1984) 149.
[25] T. Hatae, Y. Matsuzaki, S. Yamashita, Y. Yamazaki, J. Electrochem Soc. 157 (5) (2010) B650–B654.
[26] T. Klemenso, C.C. Appel, M. Mogensen, Electrochemical Solid-State Lett. 9 (9) (2006) A403–A407.
[27] D. Sarantaridis, R.J. Chater, A. Atkinson, J. Electrochem Soc. 155 (5) (2008) B467–B472.